Thermodynamic Bounds on Symmetry Breaking in Linear and Catalytic Biochemical Systems

Shiling Liang (梁师翎),[1,*] Paolo De Los Rios,[1,2] and Daniel Maria Busiello[3,†]
[1]Institute of Physics, School of Basic Sciences, École Polytechnique Fédérale de Lausanne–EPFL, 1015 Lausanne, Switzerland
[2]Institute of Bioengineering, School of Life Sciences, École Polytechnique Fédérale de Lausanne–EPFL, 1015 Lausanne, Switzerland
[3]Max Planck Institute for the Physics of Complex Systems, 01187 Dresden, Germany

(Received 4 July 2023; accepted 3 May 2024; published 31 May 2024)

Living systems are maintained out of equilibrium by external driving forces. At stationarity, they exhibit emergent selection phenomena that break equilibrium symmetries and originate from the expansion of the accessible chemical space due to nonequilibrium conditions. Here, we use the matrix-tree theorem to derive upper and lower thermodynamic bounds on these symmetry-breaking features in linear and catalytic biochemical systems. Our bounds are independent of the kinetics and hold for both closed and open reaction networks. We also extend our results to master equations in the chemical space. Using our framework, we recover the thermodynamic constraints in kinetic proofreading. Finally, we show that the contrast of reaction-diffusion patterns can be bounded only by the nonequilibrium driving force. Our results provide a general framework for understanding the role of nonequilibrium conditions in shaping the steady-state properties of biochemical systems.

DOI: 10.1103/PhysRevLett.132.228402

Introduction.—Living systems operate away from thermodynamic equilibrium, continuously harvesting and consuming energy [1]. A key feature of out-of-equilibrium living matter is the emergence of various selection phenomena, i.e., biochemical states are populated not only according to their energies, but also to kinetic features [2–7]. As a consequence, nonequilibrium settings can break equilibrium energetic symmetries, even if the intimate connection between symmetry breaking and dissipation is still elusive. Only in recent years, a growing amount of work has focused on highlighting such a link in determined contexts. For example, nonequilibrium conditions have been proven to be crucial to achieve low-error copying mechanisms that preserve DNA and RNA information with an efficiency constrained by the driving force [8–11]. Furthermore, biological systems attain high sensitivity during sensing through nonequilibrium processes [12,13], and the bistability of biochemical states, which is crucial for signaling, can be exploited only away from equilibrium [14]. Also, the newly discovered mechanism of ultra-affinity in chaperone activity is genuinely out of equilibrium and bounded by thermodynamic properties [15,16]. On a larger scale, spatial symmetry may be broken by reaction-diffusion patterns, whose emergence is associated with dissipation in the form of energy and information [17,18].

From a broader perspective, the celebrated thermodynamic uncertainty relations set a universal link between dissipation and performance of biological systems, bounding the accuracy of any stochastic current in terms of entropy production [19,20]. However, interesting features are usually not limited to the statistics of currents, as for most of the cases mentioned above.

A more general, yet not exhaustive, approach to the quest of understanding the role of dissipation in biochemical systems has been inspired by network theory. Kirchhoff's law on currents has been applied to study thermodynamic constraints in metabolic networks [21–24], and the representation of stationary states in terms of spanning trees [25,26] has been shown to be a powerful tool to derive thermodynamic and structural constraints on nonequilibrium response [27,28], and connect thermodynamics with kinetic features [29–32].

In this Letter, we give a unified description of thermodynamic bounds on nonequilibrium symmetry breaking in biochemical systems. By taking advantage of the network representation of stationary states, we derive thermodynamic bounds for the ratio of probabilities of any two states (or set of states), which is a measure of selection and, as such, a quantification of the breaking of equilibrium symmetries. We show that these bounds depend solely on network geometry and equilibrium properties, and notably not on the kinetics, as they can be determined by individual spanning trees (for which detailed balance

Published by the American Physical Society under the terms of the Creative Commons Attribution 4.0 International license. Further distribution of this work must maintain attribution to the author(s) and the published article's title, journal citation, and DOI. Open access publication funded by the Max Planck Society.

always holds). The derivation of an upper and lower bound (sandwich inequality) allows us to write down a nonequilibrium phase space, i.e., a region of the chemical space in which any feasible stationary solution must lie. These results hold for both closed and open catalytic isomerization networks described in terms of rate equations. In the case of small number of molecules or formation of complexes, our findings can be extended to chemical master equations, providing upper and lower bounds to the ratio of correlation functions of any order for general chemical reaction networks (CRN).

These thermodynamic bounds can be applied to an immense variety of symmetry-breaking mechanisms in biochemical systems. First, we rederive in a straightforward way the constraints on kinetic proofreading [8,9]. Then, we show that the contrast of reaction-diffusion (RD) patterns is limited by the thermodynamic driving force, highlighting a fascinating connection between observations and nonequilibrium conditions.

Results.—Consider a reversible catalytic isomerization network (with unimolecular and catalytic reactions) of N species whose probabilities follow a rate equation:

$$\frac{d}{dt}p_i = \sum_{j(\neq i)} (\hat{k}_{ij}p_j - \hat{k}_{ji}p_i), \tag{1}$$

where p_i is the probability of the species i, i.e., its concentration, c_i, divided by the total concentration. The transition rate from j to i might be nonlinear, i.e., $\hat{k}_{ij} = \omega_{ij}(\mathbf{p})k_{ij}$, with $\omega_{ij}(\mathbf{p}) = \omega_{ji}(\mathbf{p})$ and $\mathbf{p} = \{p_1, \ldots, p_N\}$, the instantaneous solution of Eq. (1). Here, $\omega_{ij}(\mathbf{p})$ encodes catalytic effects and k_{ij} satisfies local detailed balance, $k_{ij}/k_{ji} = e^{\beta(F_{ij}-\Delta E_{ij})}$ [33]. $\Delta E_{ij} = E_i - E_j$ is the energy difference between states i and j, and F_{ij} the nonequilibrium driving force on the edge (ij). At equilibrium, $F_{ij} = 0$ for all edges, and the stationary solution coincides with the equilibrium Boltzmann distribution, $p_i^{\mathrm{eq}} \propto e^{-\beta E_i}$. Out of equilibrium, the steady-state solution p_i^{ss} depends on nonlinear kinetics and topology of the system, not only on state energies. The nonequilibrium driving can originate from any source, e.g., chemical potential difference [8,9], thermal gradient [34,35].

When all the rates are linear, p_i^{ss} can be written in terms of spanning trees according to matrix-tree theorem [25,26]. In the nonlinear case, all steady-states satisfying $\omega_{ij}(\mathbf{p}^{\mathrm{ss}}) \neq 0, \ \forall \ i,j$ [36], can be written through the following spanning-tree decomposition

$$p_i^{\mathrm{ss}} = \mathcal{N}\sum_{\mu} A_i(T_\mu; \mathbf{p}^{\mathrm{ss}}), \tag{2}$$

where $\mathcal{N}$ is the normalization factor, and $A_i(T_\mu; \mathbf{p}^{\mathrm{ss}})$ the product of the rates of the μth spanning tree T_μ, directed toward the state i, with the sum running over all possible spanning trees. Since $A_i(T_\mu; \mathbf{p}^{\mathrm{ss}})$ depends on $\mathbf{p}^{\mathrm{ss}}$ in the nonlinear case, Eq. (2) provides a closed-form solution only for unimolecular networks, while it must be solved self-consistently in all other cases. Equation (2) can be verified by substituting it into Eq. (1).

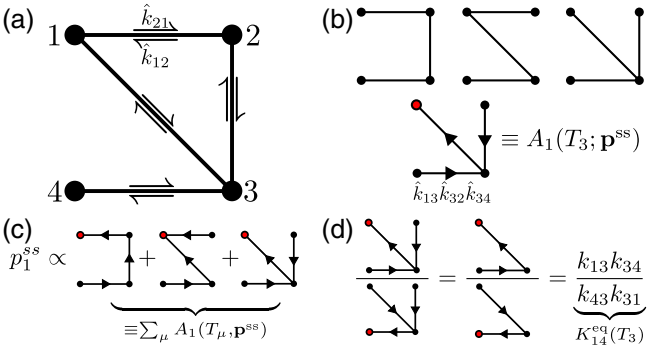


FIG. 1. (a) A four-state reaction network, where edges encode nonlinear mechanisms. (b) All spanning trees, and the directed tree to 1 from the third spanning tree. (c) Steady-state representation using directed trees. (d) The ratio of two directed trees (to state 1 and 4) obtained from the same spanning tree gives a unique reaction pathway without nonlinear terms.

To gain intuition about the relevance of spanning trees, consider the ratio $K_{ij}^{\mathrm{eq}}(T_\mu) \equiv A_i(T_\mu; \mathbf{p}^{\mathrm{ss}})/A_j(T_\mu; \mathbf{p}^{\mathrm{ss}})$. It corresponds to the product of the ratios between forward and backward rates along each edge of the reaction pathway connecting i and j and belonging to T_μ. Indeed, all edges outside this reaction pathway cancel out in the ratio. Moreover, for each T_μ, the reaction pathway connecting any two states is unique. We remark that any ratio of forward and backward transition rates along the same edge is $\hat{k}_{lm}/\hat{k}_{ml} = k_{lm}/k_{ml}$ since nonlinear terms are symmetric. Finally, due to the local detailed balance, $K_{ij}^{\mathrm{eq}}(T_\mu)$ is a pseudoequilibrium quantity, as it does not depend on the kinetics but only on thermodynamic properties. In Fig. 1, we show a simple example.

The main result of this Letter gives an upper and lower bound on the ratio of probabilities of any two stable steady-states [37,42] of a catalytic isomerization CRN, i and j, in terms of pseudoequilibrium quantities:

$$\min_{\{T_\mu\}}[K_{ij}^{\mathrm{eq}}(T_\mu)] \leq \frac{p_i^{\mathrm{ss}}}{p_j^{\mathrm{ss}}} \leq \max_{\{T_\mu\}}[K_{ij}^{\mathrm{eq}}(T_\mu)]. \tag{3}$$

The derivation relies on the implicit solution in Eq. (2), noting that nonlinearities disappear when taking ratios of forward and backward rates [42]. Naively speaking, the maximization (minimization) over all possible spanning trees amounts to maximize (minimize) over all possible reaction pathways connecting i to j. The ratio of steady-state probabilities is thus bounded from both sides by the extremal pseudoequilibrium values it can take, which are sheer thermodynamic quantities independent from

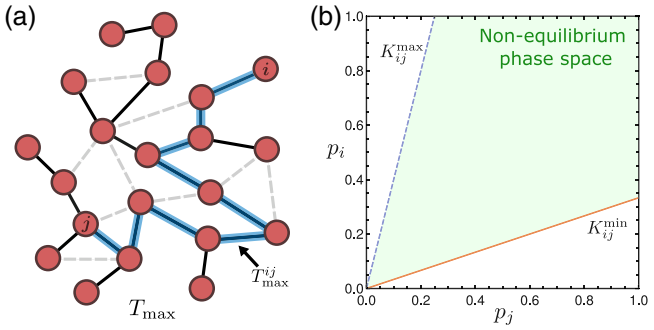


FIG. 2. (a) In black, the spanning tree providing the upper bound on $p_i^{\rm ss}/p_j^{\rm ss}$, $T_{\max}$, and its corresponding pathway $T_{\max}^{ij}$ in blue. Dashed lines represent all other edges of CRN. (b) The nonequilibrium phase space is bounded by pseudoequilibrium quantities, $K_{ij}^{\max/\min}$, evaluated from $T_{\max/\min}$.

nonlinearities of reactions and nonequilibrium kinetics [43]. However, $K_{ij}^{\rm eq}(T_\mu)$ depends on the nonequilibrium driving force along the corresponding pathway from j to i and its logarithm equals the associated entropy production into the environment [44]. As expected, at equilibrium all reaction pathways give the same contribution due to the fact that detailed balance holds, thus upper and lower bounds coincide and are both saturated. This result generalizes similar findings obtained in [45] for a specific case, and in [46] only for linear reaction networks. Below, we show that it can be further extended to sets of states, open CRN, and chemical ME.

In Fig. 2(a), we show a pictorial representation of a CRN (where edges can represent nonlinear rates), highlighting the spanning tree determining the upper bound on the symmetry breaking between $p_i^{\rm ss}$ and $p_j^{\rm ss}$, $T_{\max}$. Figure 2(b) presents (in green) the resulting nonequilibrium phase space. At equilibrium, this region collapses into a single line whose slope is determined by the Boltzmann factor $e^{-\beta\Delta E_{ij}}$. Out of equilibrium, we have $K_{ij}^{\rm eq}(T_{\max}) \equiv K_{ij}^{\max}$, and analogously we define $K_{ij}^{\min}$. These bounds determine a region in which steady-state probabilities must lie independently of their kinetic features. Noticeably, for high-dimensional spaces, the nonequilibrium phase space is a cone whose boundaries are given by bounds on ratios of all pairs of states. Conservation laws, such as mass conservation, shall be introduced as hyperplanes that reduce the accessible region and dimensionality of phase space. In presence of absolute irreversibility (e.g., unidirectional transitions), a spanning-tree representation cannot be in general obtained [47,48].

Equation (3) can be readily generalized to evaluate the selection between two groups of states $S = \{s_1, \ldots, s_N\}$ and $\Sigma = \{\sigma_1, \ldots, \sigma_M\}$, hence quantifying symmetry breaking between coarse-grained chemical macrostates. For the upper bound, we have [42]

$$\frac{\sum_{i=1}^{N} p_{s_i}^{\rm ss}}{\sum_{i=1}^{M} p_{\sigma_i}^{\rm ss}} \le \max_{\{T_\mu\}} \left(\frac{\sum_{i=1}^{N} K_{s_i s_N}^{\rm eq}(T_\mu)}{\sum_{i=1}^{M} K_{\sigma_i \sigma_M}^{\rm eq}(T_\mu)} K_{s_N \sigma_M}^{\rm eq}(T_\mu) \right), \quad (4)$$

where we (arbitrarily) selected s_N and σ_M as reference states. The lower bound can be obtained by maximizing the inverse ratio in the lhs of Eq. (4).

Open CRN.—In the most general case, chemical networks are connected to external reservoirs that keep the concentrations of some chemicals $\bar{\mathbf{c}}_m$ fixed. These couplings lead to additional terms in the rate equation:

$$\frac{d}{dt} c_i = \sum_{j(\neq i)} (\hat{k}_{ij} c_j - \hat{k}_{ji} c_i) + \sum_m (w_{im} \bar{c}_m - w_{mi} c_i), \quad (5)$$

where c_i indicates the concentrations of the species i. The spanning tree representation cannot be directly applied, as the chemostatted species are not dynamical variables. However, by merging them into a single moiety $\bar{c}_{\rm e} = \sum_m \bar{c}_m$, the effective transition rate from e to i through the transition channel m becomes $w_{im}\bar{c}_m/\bar{c}_{\rm e}$ [42]. Using this identification, the resulting rate equation can be solved with the spanning-tree approach (for steady states with nonvanishing species concentrations), substituting the normalization condition with a constraint on the fixed concentration $\bar{c}_{\rm e}$. As a consequence, the bounds shown above can be equally derived for open catalytic isomerization networks.

Kinetic proofreading.—Living systems encode information in the form of RNA and DNA. Genome duplication, translation, and transcription are processes that use this information to select the correct substrate (e.g., nucleotides, codons) with high fidelity, ensuring the survival of the organism [49]. Since the accuracy of this selection is severely limited by equilibrium constraints, Hopfield proposed the existence of energy-consuming intermediate steps that favor kinetic discrimination. The simplest nonequilibrium model for proofreading considers an enzyme E that can bind wrong (W) or right (R) substrates, forming complexes. These can be in a passive (EW and ER) or active (EW^* and ER^*) state, e.g., due to ATP hydrolysis. Therefore, the transition from passive to active complexes is driven out of equilibrium by a chemical potential $\Delta\mu$ [Fig. 3(a)]. It has been shown that the energetic cost of performing a cycle [8,9] constrains the proofreading performance, i.e., $\eta \equiv p_{EW^*}/p_{ER^*} \ge \exp[-\beta(\epsilon + \Delta\mu)]$. In its original formulation, this bound results from an optimization on reaction rates. Here, by employing the thermodynamic bounds, we have

$$\underbrace{\min_{\{T_\mu\}} \left(\frac{A_{EW^*}(T_\mu)}{A_{ER^*}(T_\mu)} \right)}_{\eta^- = \eta_\varepsilon e^{-\beta\Delta\mu}} \le \eta \le \underbrace{\max_{\{T_\mu\}} \left(\frac{A_{EW^*}(T_\mu)}{A_{ER^*}(T_\mu)} \right)}_{\eta^+ = \eta_\varepsilon e^{\beta\Delta\mu}}, \quad (6)$$

where $\eta_\varepsilon = e^{-\beta\varepsilon}$ is the equilibrium error rate due to energetic discrimination [see Fig. 3(b)]. The driving force can either increase or suppress the error rate, depending on

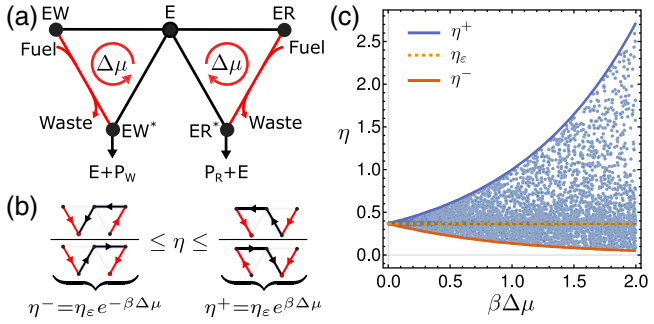


FIG. 3. (a) Proofreading network driven out of equilibrium by a chemical potential $\Delta\mu$ associated with fuel-to-waste conversion. (b) Spanning trees defining upper and lower bound of error rate, $\eta \equiv p_{EW^*}/p_{ER^*}$. (c) Blue points are error rates of the proofreading network with random kinetic parameters but the same thermodynamic bounds (red and blue lines). Dashed-yellow line shows error rate under equilibrium discrimination.

the kinetic properties of the network, as shown in Fig. 3(c). Our approach recovers the infinite-energy Hopfield rate and can be readily used to find thermodynamic bounds on multistage proofreading [42], a process with too many parameters to be bounded via optimization.

RD patterns.—Originally illustrated in the seminal work of Turing [50], the instability of the homogeneous fixed point in reaction-diffusion systems, with the consequent emergence of spatial patterns, attracted huge attention [51–53]. RD patterns have also been analyzed from a thermodynamic perspective and their onset classified as a nonequilibrium phase transition [17]. Recently, Brauns *et al.* [54] proposed a phase-space geometric approach to study pattern formation of mass-conserving reaction-diffusion systems. Consider the following dynamics for concentrations u and v:

$$\partial_t u = D_u \nabla^2 u + f(u,v),$$
$$\partial_t v = D_v \nabla^2 v - f(u,v). \tag{7}$$

The reaction term $f(u,v)$ contains all the transitions connecting u and v, i.e., $f(u,v) \equiv \sum_i (\hat{k}^{(i)}_{uv} v - \hat{k}^{(i)}_{vu} u)$, with (i) indicating the reaction channel, while D_u and D_v are diffusion coefficients. In [54], it is shown that all the values of concentrations explored by a spatially extended pattern must be embedded between the intersection of the *reactive nullcline*, $f(u,v) = 0$, and the *flux-balance subspace*, $D_u u + D_v v = \eta_0$, where η_0 is a constant determined by the *total turnover balance*. Since the reactive nullcline is determined by steady-state solutions, it must be embedded inside the nonequilibrium phase space. Here, we study which limits to RD patterns may be set only according to the laws of thermodynamics.

In Fig. 4(a), we show the system under investigation. Figure 4(b) shows, in red, the maximum and minimum accessible values of u and v in the pattern. The

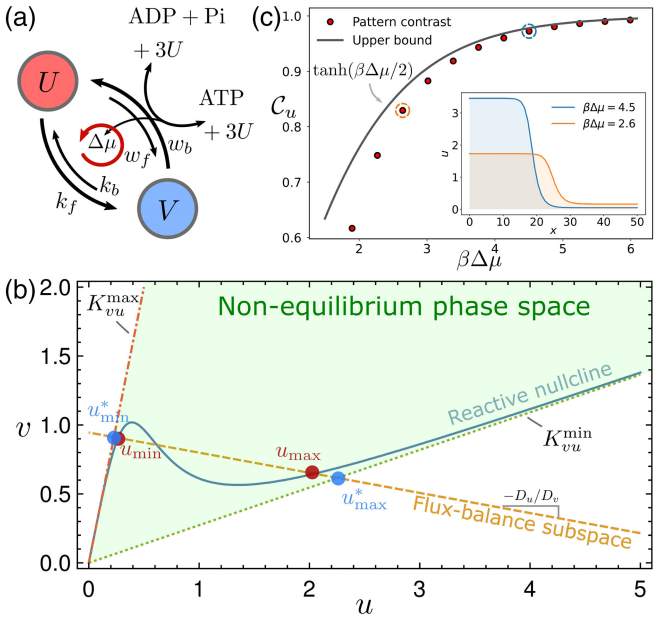


FIG. 4. Thermodynamic bound on contrast of RD patterns. (a) Model system under investigation, driven out of equilibrium by ATP hydrolysis. (b) Thermodynamic bounds (in blue) determine the nonequilibrium phase space and contain the range of the observed pattern (in red). (c) Pattern visibility is upper bounded by Eq. (9). In subpanel, we plot patterns corresponding to colored circles.

thermodynamic bounds on (u/v) at stationarity determine the nonequilibrium phase space to which the concentrations must belong. The intersections between these bounds and the flux-balance subspace define the extremal accessible values for u, $u^*_{\max/\min}$ [see Fig. 4(b)]. From [42]:

$$\frac{u_{\max}}{u_{\min}} \le \frac{u^*_{\max}}{u^*_{\min}} \le e^{\beta\Delta\mu}, \tag{8}$$

where $\beta\Delta\mu$ is the nonequilibrium driving force provided by ATP hydrolysis. The rightmost equality is reached when the system is dominated by the nonlinear pathway, while the leftmost equality is attained when $D_u/D_v \to 0$, i.e., uniform concentration of v.

At this point, we define the pattern contrast (or visibility) as $\mathcal{C}_x = (x_{\max} - x_{\min})/(x_{\max} + x_{\min})$, with $x = u,\ v$ From Eq. (8), we readily obtain [55]:

$$\mathcal{C}_u \le \tanh\left(\frac{\beta\Delta\mu}{2}\right). \tag{9}$$

This inequality immediately tells that pattern formation is a sheer consequence of nonequilibrium conditions, as at equilibrium the accessible space shrinks into a line and $\mathcal{C}_u$ goes to zero. Moreover, we only need to know the thermodynamic force driving the system out of equilibrium to bound the contrast of a pattern, independently of the

details of the kinetics. In Fig. 4(c), we numerically check Eq. (9) in our example. A tighter thermokinetic bound for $\mathcal{C}_u$ can be found by adding information about diffusion coefficients [42]. Although we inspected a simple two-state system, the presented approach is valid for any mass-conserving RD system.

Chemical ME.—CRNs with small number of molecules or formation of complexes are impossible to describe using Eq. (1). Nevertheless, it is always possible to write down a chemical ME, where each state is $\mathbf{n} = \{n_1, \ldots, n_N\}$, i.e., the number of molecules of each of the N species. Its solution can be found using the spanning-tree method in the entire chemical space. Employing the same methodology leading to Eqs. (3) and (4), we can bound the ratio between correlation functions of any order [42]. For lth order correlations, we have

$$\frac{\langle n_{i_1} \ldots n_{i_l} \rangle^{\mathrm{ss}}}{\langle n_{j_1} \ldots n_{j_l} \rangle^{\mathrm{ss}}} \leq \max_{\{T_\mu\}} \left(\frac{\sum_{\mathbf{n}} \mathbf{a}_l K^{\mathrm{eq}}_{(\mathbf{i}_l,\mathbf{a}_l),(\mathbf{i}_l,\mathbf{L})}}{\sum_{\mathbf{n}} \mathbf{a}_l K^{\mathrm{eq}}_{(\mathbf{j}_l,\mathbf{a}_l),(\mathbf{j}_l,\mathbf{L})}} K^{\mathrm{eq}}_{(\mathbf{i}_l,\mathbf{L}),(\mathbf{j}_l,\mathbf{L})} \right), \quad (10)$$

where the dependence on T_μ has been omitted for clarity. Here, $\mathbf{i}_l = (i_1, \ldots, i_l)$, $\mathbf{a}_l = (a_1, \ldots, a_l)$, and $K^{\mathrm{eq}}_{(\mathbf{i}_l,\mathbf{a}_l),(\mathbf{i}_l,\mathbf{L})}$ is evaluated from the pathway connecting the states in which $\mathbf{i}_l = \mathbf{a_l}$ and $\mathbf{i}_l = \mathbf{L}$, an (arbitrary) reference state. In [42], we show that Eq. (10) can be upper bounded by one single pathway. When $l = 1$, Eq. (10) bounds the ratio of average concentrations, as in Eq. (3). When $l = 2$, the thermodynamic bound applies to the ratio of correlations and might be useful to study how couplings inferred from correlation matrix (e.g., using a maximum-entropy approach [56–58]) depend on nonequilibrium conditions. Equation (10) is manifestly similar to Eq. (4) and the lower bound can be obtained from the inverse ratio. A detailed analysis of applications and criticalities of these thermodynamic bounds for chemical ME is left for future studies.

Discussion.—In this Letter, we derive upper and lower thermodynamic bounds on quantities that assess how much equilibrium symmetries are broken by nonequilibrium drivings. We presented two simple systems in which our framework provides interesting results, in particular highlighting the bound on pattern contrast solely as a function of the thermodynamic force. The general advantage of our findings is that they are independent of nonlinear reaction terms and kinetics, usually very important to understand systems operating away from equilibrium. As such, unraveling a reformulation of these bounds in the contexts of information thermodynamics might pave the way to understand thermodynamic constraints on chemical information-processing devices [59,60].

Countless examples of selection phenomena have proven to be relevant in as many different contexts. Surely enough, the generality of our results will be a powerful tool to understand potentialities and limitations of nonequilibrium conditions in shaping the steady-state properties of biochemical systems. Indeed, nonequilibrium drivings expand the accessible chemical space, enabling living systems to adapt to various nonlinear mechanisms and exhibit complex behaviors. For example, the emergence of chiral symmetry breaking in thermodynamically consistent CRN is an intriguing open problem in which the role of nonequilibrium conditions has not been thoroughly explored yet [61]. On theoretical grounds, our results might contribute to the promising research on sandwich inequalities [46,62,63].

Finally, the approach employed for catalytic isomerization networks might be extended to deal with CRNs represented by hypergraphs [64], underscoring the broader relevance of an accessible chemical space shaped by nonequilibrium drivings.

S. L. appreciates helpful discussions with Hong Qian and the suggestion of the visualized proof of inequality in Supplemental Material from Xiaochen Fu. S. L. and P. D. L. R. thank the Swiss National Science Foundation for support under Grant No. 200020_178763.

*shiling.liang@epfl.ch
†busiello@pks.mpg.de

[1] X. Fang, K. Kruse, T. Lu, and J. Wang, Rev. Mod. Phys. **91**, 045004 (2019).
[2] L. Bertini, A. De Sole, D. Gabrielli, G. Jona-Lasinio, and C. Landim, J. Stat. Phys. **116**, 831 (2004).
[3] T. Taniguchi and E. Cohen, J. Stat. Phys. **126**, 1 (2007).
[4] R. D. Astumian, Annu. Rev. Biophys. **40**, 289 (2011).
[5] R. D. Astumian, Nat. Commun. **10**, 1 (2019).
[6] D. M. Busiello, S. Liang, F. Piazza, and P. De Los Rios, Commun. Chem. **4**, 1 (2021).
[7] S. Amano, M. Esposito, E. Kreidt, D. A. Leigh, E. Penocchio, and B. M. Roberts, J. Am. Chem. Soc. **144**, 20153 (2022).
[8] M. Ehrenberg and C. Blomberg, Biophys. J. **31**, 333 (1980).
[9] H. Qian, J. Mol. Biol. **362**, 387 (2006).
[10] P. Sartori and S. Pigolotti, Phys. Rev. X **5**, 041039 (2015).
[11] A. A. Mohr, D. M. Busiello, S. Zamuner, and P. De Los Rios, Phys. Rev. Res. **5**, 043145 (2023).
[12] D. Hartich, A. C. Barato, and U. Seifert, New J. Phys. **17**, 055026 (2015).
[13] Y. Tu, Proc. Natl. Acad. Sci. U.S.A. **105**, 11737 (2008).
[14] M. Vellela and H. Qian, J. R. Soc. Interface **6**, 925 (2009).
[15] B. Nguyen, D. Hartich, U. Seifert, and P. De Los Rios, Biophys. J. **113**, 362 (2017).
[16] P. De Los Rios and A. Barducci, eLife **3**, e02218 (2014).
[17] G. Falasco, R. Rao, and M. Esposito, Phys. Rev. Lett. **121**, 108301 (2018).
[18] G. Nicolis and I. Prigogine, *Self-Organization in Nonequilibrium System: From Dissipative Structures to Order Through Fluctuations* (Wiley, New York, London, Sydney, Toronto, 1977).
[19] A. C. Barato and U. Seifert, Phys. Rev. Lett. **114**, 158101 (2015).
[20] J. M. Horowitz and T. R. Gingrich, Nat. Phys. **16**, 15 (2020).

[21] C. H. Schilling, S. Schuster, B. O. Palsson, and R. Heinrich, Biotechnol. Prog. **15**, 296 (1999).
[22] C. H. Schilling, D. Letscher, and B. Ø. Palsson, J. Theor. Biol. **203**, 229 (2000).
[23] D. A. Beard, E. Babson, E. Curtis, and H. Qian, J. Theor. Biol. **228**, 327 (2004).
[24] H. Qian, D. A. Beard, and S.-d. Liang, Eur. J. Biochem. **270**, 415 (2003).
[25] T. L. Hill, J. Theor. Biol. **10**, 442 (1966).
[26] J. Schnakenberg, Rev. Mod. Phys. **48**, 571 (1976).
[27] J. A. Owen, T. R. Gingrich, and J. M. Horowitz, Phys. Rev. X **10**, 011066 (2020).
[28] J. A. Owen and J. M. Horowitz, Nat. Commun. **14**, 1280 (2023).
[29] M. Polettini and M. Esposito, Phys. Rev. Lett. **119**, 240601 (2017).
[30] E. Ilker, Ö. Güngör, B. Kuznets-Speck, J. Chiel, S. Deffner, and M. Hinczewski, Phys. Rev. X **12**, 021048 (2022).
[31] F. Khodabandehlou, C. Maes, and K. Netočný, J. Stat. Phys. **189**, 41 (2022).
[32] B. Lefebvre and C. Maes, J. Stat. Phys. **190**, 90 (2023).
[33] C. Maes, SciPost Phys. Lect. Notes **32** (2021), 10.21468/SciPostPhysLectNotes.32.
[34] A. V. Dass, T. Georgelin, F. Westall, F. Foucher, P. De Los Rios, D. M. Busiello, S. Liang, and F. Piazza, Nat. Commun. **12**, 2749 (2021).
[35] S. Liang, D. M. Busiello, and P. D. L. Rios, New J. Phys. **24**, 123006 (2022).
[36] There may exist boundary steady states with vanishing concentrations that do not satisfy this condition [42]. Our derivation does not hold for these solutions.
[37] It has been conjectured that boundary states are unstable and unreachable in weakly reversible CRNs [65] and proven in different scenarios [38–41]. The stability requirement is also physically motivated.
[38] D. F. Anderson, SIAM J. Appl. Math. **71**, 1487 (2011).
[39] G. Craciun, arXiv:1501.02860.
[40] A. Deshpande and M. Gopalkrishnan, Bull. Math. Biol. **76**, 2570 (2014).
[41] D. Angeli, P. De Leenheer, and E. D. Sontag, Math. Biosci. **210**, 598 (2007).
[42] See Supplemental Material at http://link.aps.org/supplemental/10.1103/PhysRevLett.132.228402 for analytical derivations and mathematical details.
[43] The derivations of the results presented herein start from the fact that $(\sum_i a_i)/(\sum_i b_i) \leq \max(a_i/b_i)$ if a_i and b_i are positive.
[44] L. Peliti and S. Pigolotti, *Stochastic Thermodynamics: An Introduction* (Princeton University Press, Princeton, NJ, 2021).
[45] U. Cetiner and J. Gunawardena, Phys. Rev. E **106**, 064128 (2022).
[46] C. Maes and K. Netočný, Ann. Henri Poincaré **14**, 1193 (2013).
[47] M. Feinberg, *Foundations of Chemical Reaction Network Theory*, Applied Mathematical Sciences Vol. 202 (Springer International Publishing, Cham, 2019).
[48] G. Shinar and M. Feinberg, Science **327**, 1389 (2010).
[49] J. J. Hopfield, Proc. Natl. Acad. Sci. U.S.A. **71**, 4135 (1974).
[50] A. M. Turing, Phil. Trans. R. Soc. B **237**, 37 (1952).
[51] T. Biancalani, D. Fanelli, and F. Di Patti, Phys. Rev. E **81**, 046215 (2010).
[52] H. Nakao and A. S. Mikhailov, Nat. Phys. **6**, 544 (2010).
[53] M. Asllani, D. M. Busiello, T. Carletti, D. Fanelli, and G. Planchon, Phys. Rev. E **90**, 042814 (2014).
[54] F. Brauns, J. Halatek, and E. Frey, Phys. Rev. X **10**, 041036 (2020).
[55] Let $\alpha = u_{\max}/u_{\min}$, then $\mathcal{C}_u = [(\alpha-1)/(\alpha+1)] = 1 - [2/(\alpha+1)] \leq 1 - [2/(e^{\beta\Delta\mu}+1)] = \tanh(\beta\Delta\mu/2)$.
[56] W. Bialek, A. Cavagna, I. Giardina, T. Mora, E. Silvestri, M. Viale, and A. M. Walczak, Proc. Natl. Acad. Sci. U.S.A. **109**, 4786 (2012).
[57] M. Castellana and W. Bialek, Phys. Rev. Lett. **113**, 117204 (2014).
[58] A. De Martino and D. De Martino, Heliyon **4**, e00596 (2018).
[59] S. Amano, M. Esposito, E. Kreidt, D. A. Leigh, E. Penocchio, and B. M. Roberts, Nat. Chem. **14**, 530 (2022).
[60] S. Flatt, D. M. Busiello, S. Zamuner, and P. De Los Rios, Commun. Phys. **6**, 205 (2023).
[61] D. G. Blackmond, Angew. Chem., Int. Ed. **48**, 2648 (2009).
[62] S. Liang and S. Pigolotti, Phys. Rev. E **108**, L062101 (2023).
[63] G. Manzano, G. Kardeş, É. Roldán, and D. Wolpert, Phys. Rev. X **14**, 021026 (2024).
[64] S. Dal Cengio, V. Lecomte, and M. Polettini, Phys. Rev. X **13**, 021040 (2023).
[65] M. Feinberg, Chem. Eng. Sci. **42**, 2229 (1987).